BEFIB2012 – Fibre reinforced concrete
Joaquim Barros et al. (Eds)
 UM, Guimarães, 2012

THE PREDICTIVE PERFORMANCE OF DESIGN MODELS FOR THE PUNCHING RESISTANCE OF SFRC SLABS IN INNER COLUMN LOADING CONDITIONS

Bernardo N.M. Neto[*], Joaquim A.O. Barros[†] and Guilherme S. Melo[†]

[*] Dep. Civil Eng., School Eng., University of Minho / University of Brazilia-UnB
Campus de Azurém 4800-058 Guimarães, Portugal
e-mail: bnmn@hotmail.com

[†] Dep. Civil Eng., School Eng., University of Minho
Campus de Azurém 4800-058 Guimarães, Portugal
e-mail: barros@civil.uminho.pt, web page

[†] Dep. Civil Eng., School Eng., University of Brasília-UnB
Campus Universitario Darcy Ribeiro 70910-900 Brazilia, Brazil
e-mail: melog@unb.br

Keywords: Punching, steel fibre reinforced concrete, slabs, analytical models.

Summary: *In the recent years steel fibre reinforced concrete (SFRC), in a volume percentage between 0.75 and 1.25, is being proposed to build slabs supported on piles and slabs supported on columns, where the unique conventional reinforcement is composed of some steel bars in the alignments of the columns/piles, designated as anti-progressive collapse bars.*

Punching resistance, however, can be a concern in this structural system. In fact, punching has a brittle failure character, and the prediction of the punching resistance is still a challenge, even in concrete slabs with traditional reinforcement systems. The difficulties on assessing the contribution of the reinforcement mechanisms of steel fibres for the flexural and shear resistance in the critical punching perimeter increase this complexity.

The research carried out in this paper has the purpose of assessing the reliability of existing analytical models for the prediction of the punching resistance of SFRC slabs. For this purpose, a data-base of experimental tests with SFRC slabs failing in punching was built and the predictive performance of four analytical available models was assessed. In order to turn more practical the model that is more reliable from physical and mechanical point of views, the concepts proposed by Model Code 2010 for the characterization of the post-cracking behaviour of FRC were introduced in this model.

1 INTRODUCTION

Slabs on grade is the most common application of steel fibre reinforced concrete (SFRC), since the high static indeterminacy of this type of structural elements is favourable to the activation of the fibre reinforcement mechanisms in several zones, resulting in high levels of stress redistribution with consequent benefits in terms of load carrying and energy dissipation capacities [1]. In this application the content of steel fibres, in general, does not exceed 30 kg/m^3 of concrete, depending on the properties of the soil and load conditions [2, 3]. Due to the stress redistribution capacity provided by fibre reinforcement, the use of SFRC has been extended to continuous slabs supported on piles, and, more recently, to continuous slabs supported on columns, where contents of steel fibres between 50 and 100 kg/m^3 have been applied [4-6]. This type of slabs is generally designated by Elevated Steel Fibre Reinforced Concrete (ESFRC) slab, and it includes a minimum continuity bars, also referred as anti-progressive collapse bars, placed in the bottom of the slab in the alignment of the columns in both directions [7].

Since the flexural capacity of ESFRC slabs is almost provided by steel fibre reinforcement, flexural failure

modes are, in general, the governing ones, but punching resistance needs to be evaluated since in certain loading conditions punching failure can occur, which should be avoided due to its brittle nature [8].

To predict the punching resistance of ESFRC slabs some models have been proposed [9-12], but the calibration process of the parameters of these models is, in general, executed by using a relatively small number of experimental data. This strategy can conduct to a quite different predictive performance of these models, when a large data-base is used for this purpose. To estimate the reliability of these models, in the present work a data-base was built including the relevant experimental results available in the literature dealing with the punching resistance of SFRC slabs. Using the punching resistance recorded experimentally, V_{exp}, and determining the punching resistance predicted by the selected theoretical models, V_{the}, (they have in general an empirical or a semi-empirical nature) the predictive performance of these models is analyzed and discussed in the present work. The model that integrates in a more comprehensive and rational basis the contribution of fibre reinforcement, requires, however, the knowledge of the stress-crack width (σ-w) relationship obtained from direct tensile tests. To simplify this process, the σ-w was derived from the recommendations of the Model Code 2010 [13] and taking into account available experimental data for the characterization of the post-cracking residual strength of SFRC.

2 THEORETICAL MODELS

The first model (herein designated by M1) considered in the present work is the one proposed by Shaaban and Gesund [9] that has a formulation based on the equation recommended by ACI [14]:

$$V_u = 0.6 \cdot \left(0.025 \cdot W_f + 0.567\right) \cdot b_0 \cdot d \cdot \sqrt{f_c} \ \text{[MPa, mm]} \tag{1}$$

where

$$b_0 = 4 \cdot \left(c + d\right) \ \text{[mm]} \tag{2}$$

is the critical punching perimeter (Figure 1), d is the internal arm of the flexural reinforcement of the slab, f_c is the average value of the concrete compressive strength, c is the edge of the square cross section of the column, and

$$W_f = \frac{7850 \cdot V_f}{w_c} = \frac{7850 \cdot V_f}{2400} = 3.27 \cdot V_f \tag{3}$$

is the relationship between the weight percentage (W_f) and the volume percentage (V_f) of steel fibres.

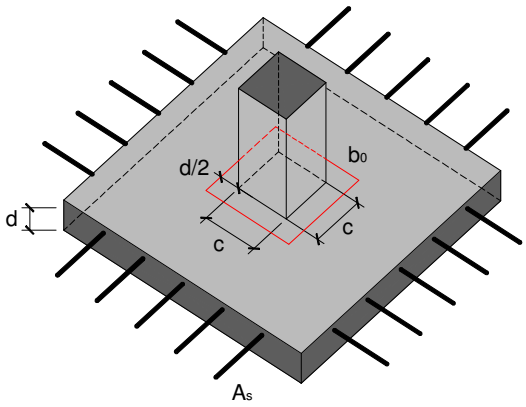

Figure 1: Geometric variables involved in the analytical formulations to estimate the punching resistance of a reinforced concrete slab.

The second model (herein designated by M2) is the one published by Harajli *et al.* [10] that have proposed

the following equation to quantify the contribution of steel fibres for the punching resistance of a SFRC slab:

$$\Delta V_u = \left(0.033 + 0.075 \cdot V_f\right) \cdot b_0 \cdot d \cdot \sqrt{f_c} \quad \text{[MPa, mm]} \tag{4}$$

In this work the authors have added ΔV_u to the equation recommended by ACI [14] for the evaluation of the punching resistance of a RC slab. The meaning of the symbols in Eq. (4) is the same of those adopted in Eq. (1).

The third model (herein designated by M3) is the one proposed by Holanda [11] that has included in the equation developed by Alexander and Simmonds [15] a parcel that intends to simulate the contribution of fibre reinforcement for the punching resistance of RC slabs, having resulted the following equation:

$$V_u = 0.0035 \cdot d \cdot \sqrt{c \cdot d \cdot f_c \cdot \frac{\rho_{sl} \cdot f_{sy}}{f_c} \cdot \left(170 - \frac{\rho_{sl} \cdot f_{sy}}{f_c}\right) \cdot \left(0.15 \cdot V_f + 0.51\right) \cdot \sqrt{f_c}} \quad \text{[MPa, cm, \%]} \tag{5}$$

where ρ_{sl} is the ratio of the flexural reinforcement, and f_{sy} is its yield stress.

The last model (herein designated by M4), whose predictive performance is analyzed in the present work, is based on the "critical shear crack theory" proposed by Muttoni and Ruiz [12] for the evaluation of the punching resistance of RC slabs (Figure 2). According to this theory, the punching resistance of a SFRC slab is obtained from:

$$V_{Rd} = V_{Rd,c} + V_{Rd,f} \tag{6}$$

where $V_{Rd,c}$ is the design value of the contribution of the concrete matrix that can be obtained according to the recommendations of [8], and $V_{Rd,f}$ is the contribution of the design post-cracking residual tensile strength provided by fibre reinforcement mechanisms.

$$V_{Rd,f} = \int_{A_p} \sigma_{tfd}(w) \cdot dA_p \tag{7}$$

being A_p the horizontal projection of the failure surface, and $\sigma_{tfd}(w)$ is the design value of the pos-cracking residual tensile strength of a SFRC that depends on the crack width (w).

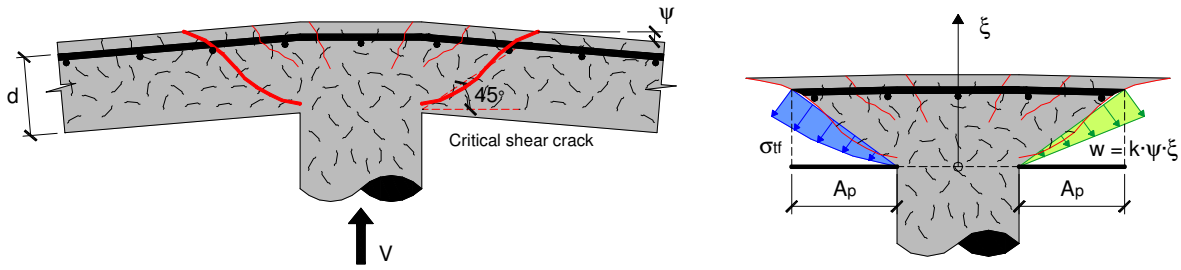

Figure 2: Assumed distribution of crack width and tensile stress due to fibre reinforcement along the failure surface, according to the critical shear crack theory (adapted from [12]).

Adopting a simplified approach where the crack width is obtained from the rotation of the slab outside the column region (ψ, Figure 2) and from the distance ξ of the soffit of the slab:

$$w(\psi, \xi) = k \,.\, \psi \,.\, \xi \tag{8}$$

and considering the "Variable Engagement Model – VEM" proposed by Voo and Foster [16] for the evaluation of the $\sigma_{tf}(w)$:

$$\sigma_N(w) = \frac{1}{\pi}.\arctan\left(\frac{w}{\alpha_1.\ell_f}\right).\left(1-\frac{2.w}{\ell_f}\right)^2.\frac{\ell_f}{d_f}.V_f.\tau_b \tag{9a}$$

$$\sigma_{tf}(w) = k_{ek}.\sigma_N(w) \tag{9b}$$

$$\sigma_{tfd}(w) = \frac{\sigma_{tf}(w)}{\gamma_f} = \frac{1}{\gamma_f}.\frac{k_{ek}}{\pi}.\arctan\left(\frac{w}{\alpha_1.\ell_f}\right).\left(1-\frac{2.w}{\ell_f}\right)^2.\frac{\ell_f}{d_f}.V_f.\tau_b \tag{9c}$$

it is obtained, after some assumptions, the following simplified equation:

$$V_{Rd,f} = \int_{A_p}\sigma_{tfd}(\psi,\xi)\cdot dA_p = A_p\cdot\sigma_{tfd}(\psi,h_c) \tag{10}$$

where h_c is a control distance from the soffit of the slab at which the average stress is obtained. Muttoni and Ruiz [12] verified that adopting $h_c=d/3$ has allowed the model to predict with good agreement some experimental results, leading to a further simplification for Eq. (10):

$$V_{R,f} = A_p\cdot\sigma_{tf}\left(w=\frac{\psi\cdot d}{6}\right) \tag{11}$$

In Eq. (9) l_f and d_f are the fibre length and diameter, respectively, α_1 is a parameter that depends on the fibre aspect ratio (l_f/d_f):

$$\alpha_1 = \frac{d_f}{3.5\cdot l_f} \tag{12}$$

τ_b is a parameter that provides the fibre bond strength:

$$\tau_b = \begin{cases} 0.8\ f_c^{0.5} & for\ "hooked\ ends"\ fibres \\ 0.6\ f_c^{0.5} & for\ "crimped"\ fibres \\ 0.4\ f_c^{0.5} & for\ "straight"\ fibres \end{cases} \tag{13}$$

and K_{ek} is a parameter that is obtained by calculating the 5% percentile of the $\sigma_{Nti}/\sigma_{Nci}$ for a number of crack widths (1, 2 and 3 mm, Figure 3a) and attributing to K_{ek} the minimum value of them, where σ_{Nti} and σ_{Nci} are the residual tensile strength at the i^{th} crack width (in mm) registered in experimental tests and by the application of Eq. (9a), respectively.

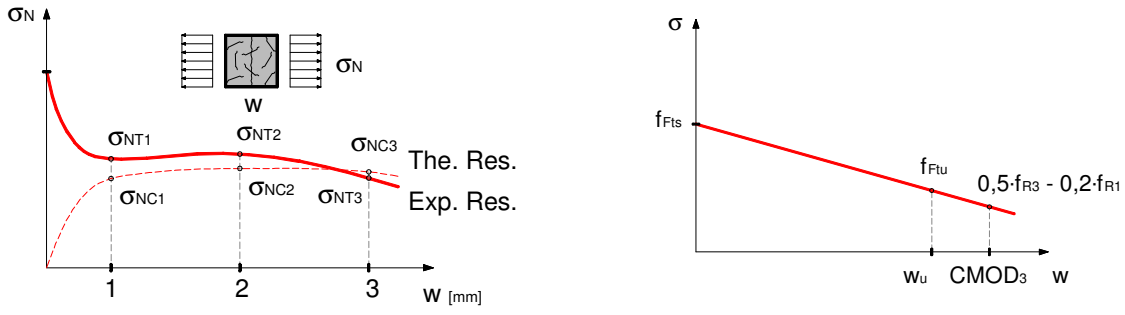

a) b)

Figure 3: a) Evaluation of K_{ek} [16]; b) stress-crack opening relationship proposed by Model Code 2010 [13].

Due to the difficulty of obtaining $\sigma_{tfd}(w)$ from equation (9c), since it requires the execution of uniaxial tensile tests to determine the K_{ek} parameter, and few experimental data is available that can be directly used in the equation (9a), another alternative is explored for the evaluation of $\sigma_{tfd}(w)$. For this purpose, the most recent recommendations of Model Code 2010 [13] were used, and the $\sigma_{Nt}(w)$ is derived from the data obtained in standard notched beam bending tests for the characterization of the post-cracking behaviour of FRC. Figure 3b) represents this stress-crack width diagram that is defined from the concept of residual strength parameter f_{Ri}. To determine f_{Ri} three point notched FRC beam bending tests are executed (Figure 4a) and the typical obtained force (F) *versus* crack mouth opening displacement ($CMOD$) relationship, represented in Figure 4b, is used for this purpose.

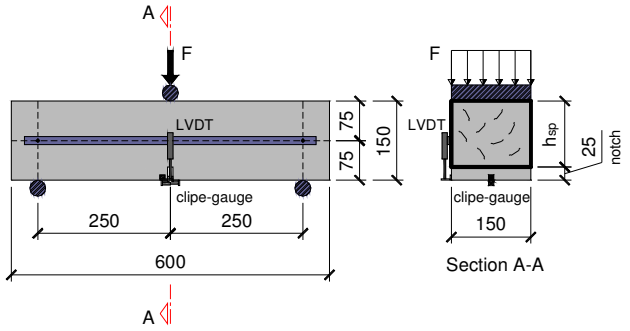

a)

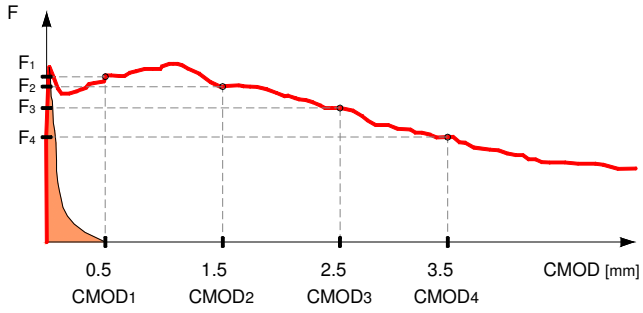

b)

Figure 4: Three point notched beam bending test for the characterization of the post-cracking behaviour of FRC: a) test setup (dimensions in mm); b) Typical F – CMOD curve [12].

Therefore, based on the force values for the $CMOD_j$ (j= 1 to 4, see Figure 4b), the corresponding force values, F_j, are obtained, and the derived residual flexural tensile strength parameters are determined from the following equation:

$$f_{R,j} = \frac{3 \cdot F_j \cdot L}{2 \cdot b \cdot h_{sp}^{\ 2}} \tag{14}$$

where f_{Rj} [N/mm^2] and F_j [N] are, respectively, the residual flexural tensile strength and the load corresponding to $CMOD = CMOD_j$ [mm]. Using f_{R1} and f_{R3}, the stress-crack width diagram represented in Figure 3b) can be determined,

$$f_{Fts} = 0.45 \cdot f_{R1} \tag{15}$$

$$f_{Ftu} = f_{Fts} - \frac{w_u}{CMOD_3}(f_{Fts} - 0.5 \cdot f_{R3} + 0.2 \cdot f_{R1}) \geq 0 \tag{16}$$

where w_u is the maximum crack opening accepted in structural design that depends on the required ductility, but should not exceed 2.5 mm.

In the major part of the experimental tests composing the built data-base for the punching of SFRC slabs, hooked ends steel fibres were used in a volume percentage that was smaller than 2%. The f_{Rj} values are dependent, not only of the material and geometric characteristics of the fibres, but also on the properties of the surrounding cement matrix. However, to derive simple equations for the estimation of f_{Rj} it is believed that fibre volume is the most influent parameter. Therefore, to derive equations for the evaluation of f_{R1} and f_{R3} from the fibre volume percentage, V_f, a data base composed of 69 results was collected [17]. In Figure 5 is represented the $\lambda_i=f_{Ri,exp}/f_{Ri,the}$ versus V_f, where $f_{Ri,exp}$ and $f_{Ri,the}$ are the residual parameters obtained experimentally and those determined from the following equations:

$$f_{R1} = k_1 \cdot V_f = 7.0 \cdot V_f \quad \text{[MPa, \%]} \tag{17a}$$

$$f_{R3} = k_2 \cdot V_f = 5.5 \cdot V_f \quad \text{[MPa, \%]} \tag{17b}$$

$$f_{R3} = k_3 \cdot f_{R1} = 0.8 \cdot f_{R1} \quad \text{[MPa]} \tag{17c}$$

where the values of k_1 and k_2 parameters were derived in order to assure a relatively small percentage (5% was considered an appropriate value for this purpose) of λ_i results that are extremely dangerous (λ_i <0.75) and dangerous ($\lambda_i \in$[0.75-0.9]) according to an adjusted version of the "Demerit Points Classification" (DPC) model proposed by Collins [18]. Figure 5a presents the λ_i-V_f, Figure 5b illustrates for f_{Ri} the lower quartile (Q1), median (Q2), upper quartile (Q3) and the extreme values (minimum and maximum), while Figure 5c shows the percentage of λ_i values higher and lesser than 1.0. Figure 5a shows a tendency for a smaller dispersion of the λ_i with the increase of V_f. As expected, Figure 5b evidence a higher dispersion for f_{R3} than for f_{R1}, but the average value of λ_1 and λ_3 is in the interval 1 to 1.5 and the Q1 and Q3 are around the limits of 1 and 1.5, respectively, giving confidence on the use of the simple equation (17).

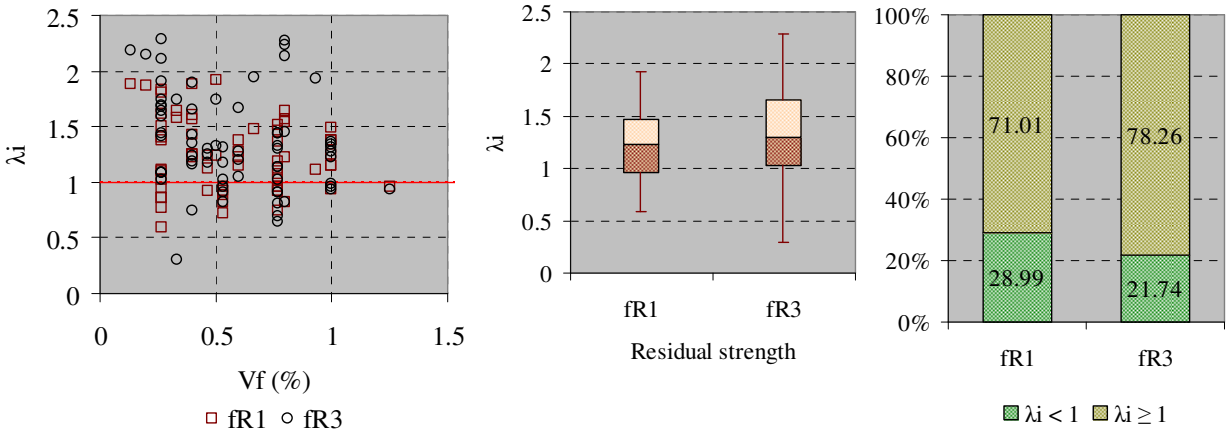

Figure 5: a) Representation of λ_i-V_f, b) box and whiskers representation of the λ_i, and c) representation of the percentage of λ_i values higher and lesser than 1.0.

3 PREDICTIVE PERFORMANCE OF THE SELECTED MODELS

3.1 Data-base assembly

The collected data-base (DB) is composed by 142 tested slabs, 125 of them were reinforced with longitudinal steel bars/grids in order to avoid the occurrence of flexural failure modes. None of these slabs have conventional shear/punching reinforcement. However, 105 slabs composing the DB were made by SFRC. In terms of concrete

compressive strength, f_{cm}, the DB is composed of slabs with f_{cm} in the range 14 to 93 MPa, so a quite high interval exists for a parameter that has a relevant impact on the punching resistance of concrete slabs. For the slabs that were flexurally reinforced with steel bars, the internal arm of this reinforcement (d, Figure 2) has varied from 14 mm to 180 mm, while the reinforcement ratio (ρ_{sl}) is in the interval 0 to 2.75%. In the SFRC slabs, "*hooked*", "*twisted*", "*crimped*", "*corrugated*", "*paddle*" and "*Japanese*" type of fibres were used, with an aspect-ratio that varied from 20 to 100, and in a volume percentage ≤2%. In some of the SFRC slabs (6 specimens), the SFRC was only applied in a region around the loaded area (that represents the position of the column), considered the region where punching failure mechanism can occur. In terms of loading conditions, all the slabs of the DB were submitted to a load distributed in a certain area of the slab without transferring any bending moments form the loading device to the slab. In the tests of the DB, the columns were simulated by a RC element monolithically connected to the slab, or applying steel plates, or even a semi-spherical device in between the piston of the actuator and the tested slab. Several cross sections were adopted when using RC elements or steel plates: square, and circular. To avoid results that can compromise the reliability of this statistical analysis, the slabs with a thickness lower than 80 mm were discarded, since an eventual influence of size effect can have a detrimental consequence on this study. Furthermore, the slabs where the concrete compressive strength was decreased more than 15 % in consequence of the addition of fibres were also neglected, since this decrease reveals that the SFRC mix composition was not properly designed.

3.2 General statistical analysis procedures

The performance of the selected models for the prediction of the punching resistance of SFRC slabs is appraised using the collected data registered in the DB. For each described model (M1 to M4), the obtained values of V_{the} are compared with V_{exp} and a χ factor corresponding to the V_{exp}/V_{the} ratio is evaluated. On the performed analysis V_{the} includes all the parcels that contribute for the punching resistance according to the corresponding model. In the evaluation of V_{the} average values for the properties of the intervening materials were considered in order to assure that χ>1.0 represents a safety result from the fundamental point of view of the average properties of the materials and the behaviour of the tested slabs. In the formulations were safety factors are used, they were considered as unitary values for the present purpose.

3.3 Analysis of the obtained results

The results are analyzed in terms of $\chi=V_{exp}/V_{the}$ parameter, the minimum and the maximum values, and the lower, median and upper quartiles, Q1, Q2 and Q3, respectively. The results were also analyzed considering an adapted version of the DPC [18] according to the criteria indicated in Table 1.

Table 1: Demerit points classification (DPC) criteria for χ

$\chi=V_{exp}/V_{the}$	Classification	Penalty
< 0.50	Extremely Dangerous	10
[0.50-0.85[	Dangerous	5
[0.85-1.15[	Appropriate Safety	0
[1.15-2.00[	Conservative	1
≥ 2.00	Extremely Conservative	2

Figure 6a shows the percentage of χ higher and lesser than 1.0 for the analyzed models, while the corresponding box and whiskers are represented in Figure 6b. It can be concluded that M3 model provides the minimum percentage of values of χ<1.0. Table 2 presents the obtained results in terms of average (Avg), standard deviation (STD) and coefficient of variation (COV) for the χ. This table and Figure 6b evidence that M4 model assures the average value of χ (χ_{med}) closest to the unity, with the smallest STD and COV values (χ_{STD}, χ_{COV}).

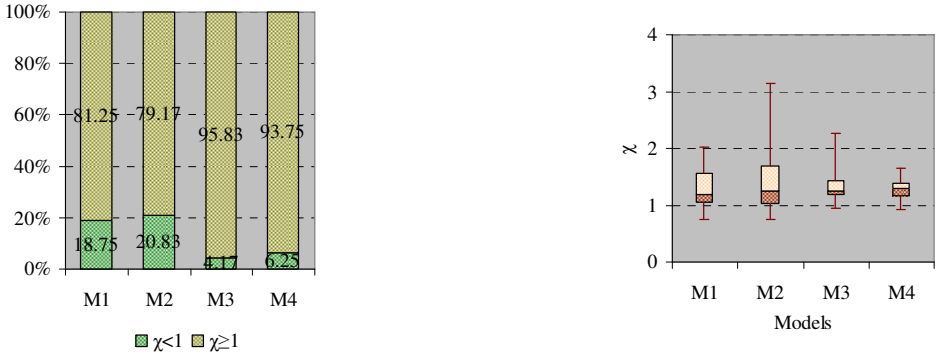

Figure 6: a) Percentage of χ higher and lesser than 1.0, b) "box and whiskers" representation.

Table 2: Average, standard deviation (STD) and coefficient of variation (COV) of χ based on a DPC classification

Classification in terms of DPC								
Model	M1		M2		M3		M4	
χ	N° slabs	Penal.	N° slabs	Penal.	N° slabs	Penal.	N° slabs	Penal.
< 0.50	0	0	0	0	0	0	0	0
[0.50-0.85[	3	15	5	25	0	0	0	0
[0.85-1.15[	17	0	16	0	9	0	11	0
[1.15-2.00[	27	27	20	20	36	36	37	37
≥ 2.00	1	2	7	14	3	6	0	0
Total	48	44	48	59	48	42	48	37
Statistical resume								
Model	M1		M2		M3		M4	
Average (Avg)	1.29		1.44		1.36		1.27	
STD	0.34		0.62		0.31		0.16	
COV (%)	26.00		42.90		22.69		12.37	

Influence of the fibre volume percentage

To evaluate the influence of the fibre volume percentage, V_f, on the χ_{avg} and on the dispersion of the results, three classes were considered, $V_f \leq 0.6$, $0.6 < V_f \leq 1.2$, $V_f > 1.2$, since the intermediate class corresponds to the current application of steel fibres for the punching resistance of concrete slabs. Figure 7 presents the obtained results. In general, χ_{avg} becomes closer to the unit value with the increase of V_f. The minimum dispersion of results is registered for the class of higher V_f. M4 Model presented χ_{avg} values closer to the unit value for all the V_f classes, as well as the smallest COVs.

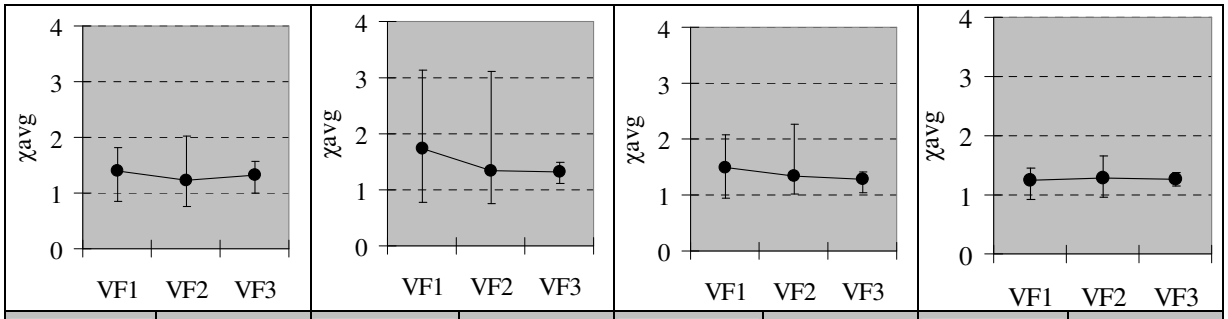

χ_{avg}(VF1)=1.40	COV(VF1)=25.41%	χ_{avg}(VF1)=1.74	COV(VF1)=46.21%	χ_{avg}(VF1)=1.49	COV(VF1)=28.65%	χ_{avg}(VF1)=1.25	COV(VF1)=15.79%
χ_{avg}(VF2)=1.23	COV(VF2)=28.79%	χ_{avg}(VF2)=1.33	COV(VF2)=43.08%	χ_{avg}(VF2)=1.33	COV(VF2)=20.43%	χ_{avg}(VF2)=1.29	COV(VF2)=12.62%
χ_{avg}(VF3)=1.31	COV(VF3)=14.62%	χ_{avg}(VF3)=1.32	COV(VF3)=8.97%	χ_{avg}(VF3)=1.27	COV(VF3)=10.35%	χ_{avg}(VF3)=1.27	COV(VF3)=5.91%
a) M1		b) M2		c) M3		d) M4	

VF1- $V_f \leq 0.6$; VF2- $0.6 < V_f \leq 1.2$; VF3- $V_f > 1.2$

Figure 7: Influence of the fibre volume percentage on the χ_{avg}.

Influence of the fibre aspect ratio

The DB was organized in order to assess the influence of the fibre aspect ratio (E= l_f/d_f) on the average value of χ (χ_{avg}). For this purpose three groups were formed: E1- $l_f/d_f \leq 50$; E2- $50 < l_f/d_f \leq 70$; E3- $l_f/d_f > 70$. Figure 8 presents the obtained results, where it is visible that χ_{avg} was higher than 1 in all the models, regardless the fibre aspect ratio, and the dispersion of χ_{avg} has, in general, increased with the fibre aspect ratio. This figure also reveals that M4 provides the χ_{avg} values that are, in general, closer to the unit and with the lowest COVs.

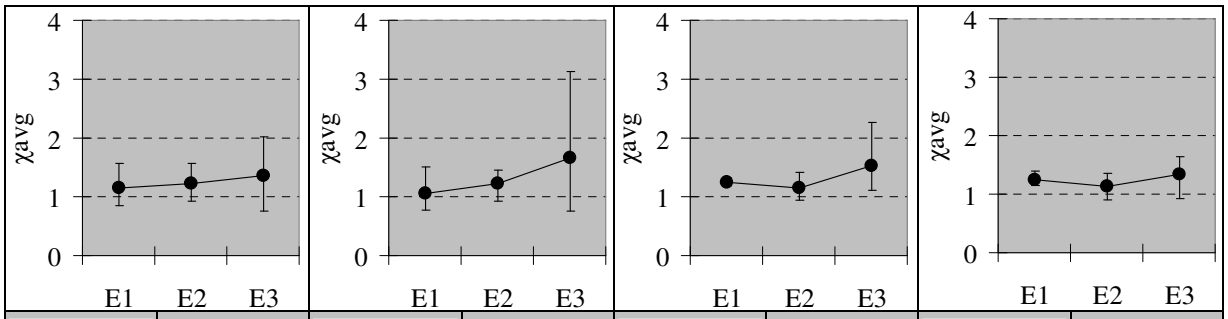

χ_{avg}(E1)=1.15	COV(E1)=26.27%	χ_{avg} (E1)=1.06	COV(E1)=29.20%	χ_{avg} (E1)=1.24	COV(E1)=4.51%	χ_{avg} (E1)=1.25	COV(E1)=7.06%
χ_{avg}(E2)=1.23	COV(E2)=15.62%	χ_{avg} (E2)=1.22	COV(E2)=12.18%	χ_{avg} (E2)=1.15	COV(E2)=11.44%	χ_{avg} (E2)=1.14	COV(E2)=13.54%
χ_{avg}(E3)=1.36	COV(E3)=29.35%	χ_{avg} (E3)=1.67	COV(E3)=45.16%	χ_{avg} (E3)=1.52	COV(E3)=21.83%	χ_{avg} (E3)=1.34	COV(E3)=10.41%
a) M1		b) M2		c) M3		d) M4	

E1- $l_f/d_f \leq 50$; E2- $50 < l_f/d_f \leq 70$; E3- $l_f/d_f > 70$

Figure 8: Influence of the fibre aspect ratio on the χ_{avg}.

Influence of the concrete compressive strength

To assess the influence of the average compressive strength of SFRC, f_{cm}, on the χ_{avg} and on the dispersion of the results, three classes were considered, $f_{cm} \leq 30$ MPa, $30 < f_{cm} \leq 50$ MPa, $f_{cm} > 50$ MPa, since the intermediate class corresponds to the current application of steel fibres for the punching resistance of concrete slabs. Figure 9 presents the obtained results. M4 Model presented χ_{avg} values closer to the unit value for almost all the f_{cm} classes, as well as the smallest COVs.

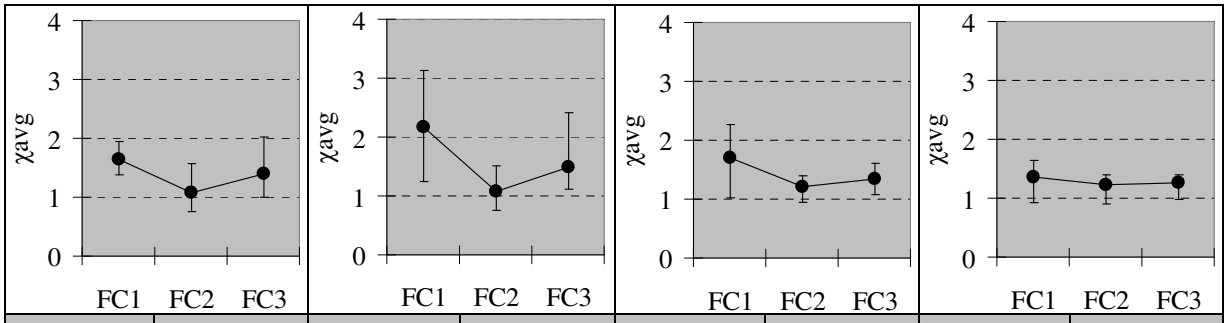

χ_{avg}(FC1)=1.65	COV(FC1)=11.41%	χ_{avg}(FC1)=2.16	COV(FC1)=29.45%	χ_{avg}(FC1)=1.69	COV(FC1)=23.85%	χ_{avg}(FC1)=1.35	COV(FC1)=14.95%
χ_{avg}(FC2)=1.08	COV(FC2)=19.53%	χ_{avg}(FC2)=1.07	COV(FC2)=20.27%	χ_{avg}(FC2)=1.21	COV(FC2)=8.97%	χ_{avg}(FC2)=1.23	COV(FC2)=11.34%
χ_{avg}(FC3)=1.40	COV(FC3)=22.88%	χ_{avg}(FC3)=1.48	COV(FC3)=29.38%	χ_{avg}(FC3)=1.33	COV(FC3)=13.47%	χ_{avg}(FC3)=1.26	COV(FC3)=10.64%
a) M1		b) M2		c) M3		d) M4	

FC1- $f_{cm}\leq$30 MPa; FC2- 30<$f_{cm}\leq$50 MPa; FC3- f_{cm}>50 MPa

Figure 9: Influence of the average concrete compressive strength on the χ_{avg}.

Influence of the flexural reinforcement ratio

To evaluate the influence of the flexural reinforcement ratio, ρ_{sl}, on the χ_{avg} and on the dispersion of the results, three classes were considered, $\rho_{sl}\leq$0.6, 0.6<$\rho_{sl}\leq$1.2, ρ_{sl}>1.2, since the largest number of cases in the DB corresponds to the intermediate class. Figure 10 presents the obtained results. In general, χ_{avg} becomes closer to the unit value with the increase of ρ_{sl}. The COV values have a tendency to decrease with the increase of ρ_{sl}. M4 Model presented χ_{avg} values closer to the unit value for almost all the ρ_{sl} classes, as well as the smallest COVs.

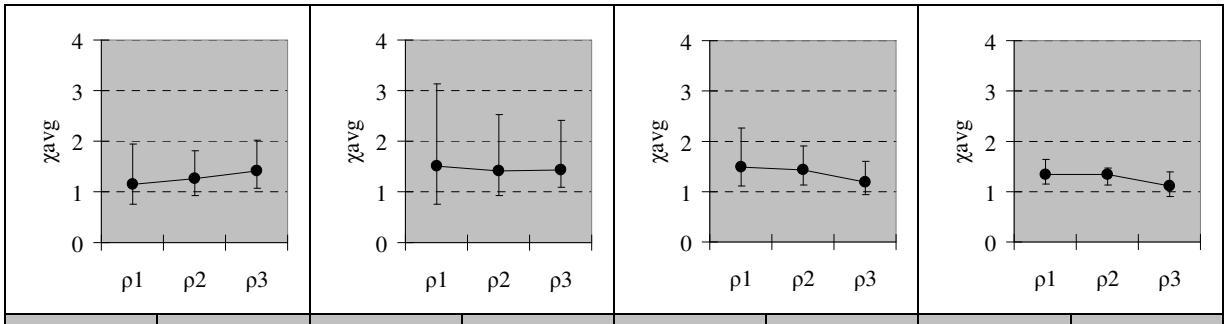

χ_{avg}(ρ1)=1.15	COV(ρ1)=42.62%	χ_{avg}(ρ1)=1.52	COV(ρ1)=71.47%	χ_{avg}(ρ1)=1.49	COV(ρ1)=30.09%	χ_{avg}(ρ1)=1.34	COV(ρ1)=11.54%
χ_{avg}(ρ2)=1.26	COV(ρ2)=23.70%	χ_{avg}(ρ2)=1.41	COV(ρ2)=36.65%	χ_{avg}(ρ2)=1.44	COV(ρ2)=17.42%	χ_{avg}(ρ2)=1.34	COV(ρ2)=6.42%
χ_{avg}(ρ3)=1.42	COV(ρ3)=16.19%	χ_{avg}(ρ3)=1.44	COV(ρ3)=23.62%	χ_{avg}(ρ3)=1.18	COV(ρ3)=16.43%	χ_{avg}(ρ3)=1.12	COV(ρ3)=13.53%
a) M1		b) M2		c) M3		d) M4	

ρ1- $\rho_{sl}\leq$0.6; ρ2- 0.6<$\rho_{sl}\leq$1.2; ρ3 - ρ_{sl}>1.2

Figure 10: Influence of the flexural reinforcement ratio on the χ_{avg}.

4 CONCLUSIONS

In this work the predictive performance of four published models for the evaluation of the punching resistance of steel fibre reinforced concrete (SFRC) slabs was assessed by using the data-base (DB) composed by 142 experimentally tested slabs. The formulations were briefly described and the model recommended by Muttoni and Ruiz was adapted in order to avoid the necessity of using experimental data from direct tensile tests with SFRC for the evaluation of the contribution of steel fibres for the punching resistance of concrete slabs. In

this context, this experimental data was indirectly assessed by adopting the stress-crack width relationship proposed by Model Code 2010, and deriving the parameters that define this relationship from simple equations supported on available experimental data obtained from three point notched SFRC beam bending tests.

Considering $\chi=V_{exp}/V_{the}$ as the relevant parameter for the assessment of the predictive performance of the considered models, where V_{exp} and V_{the} are the punching resistance recorded experimentally and from the models, it was verified that the Muttoni and Ruiz model has assured the average value of χ closest to the unity, with the smallest STD and COV values amongst the four analyzed models. In the evaluation of V_{the} average values for the properties of the intervening materials were considered, and safety factors were not considered. The DB was also analyzed in terms of assessing the influence of the fibre volume percentage, fibre aspect ratio, average SFRC compressive strength and the flexural reinforcement ratio on the χ and COV values. For all these parameters, and regardless the sub-classes considered, the Muttoni and Ruiz model has, in general, conducted to values of χ closest to the unit, as well as to the smallest COVs, so it is the model recommended for the evaluation of the punching resistance of SFRC slabs.

ACKNOWLEDGEMENTS

The study presented in this paper is a part of the research project titled "SlabSys-HFRC - Flat slabs for multi-storey buildings using hybrid reinforced self-compacting concrete: an innovative structural system", with reference number of PTDC/ECM/120394/2010. The first author acknowledges the support provided by the CAPES and CNPq grant.

REFERENCES

[1] Barros, J.A.O.; Figueiras, J.A., "Experimental behaviour of fiber concrete slabs on soil", Journal Mechanics of Cohesive-frictional Materials, 3, 277-290, 1998. http://hdl.handle.net/1822/13517.
[2] Barros, J.A.O.; Gouveia, A.V.; Sena-Cruz, J.M.; Azevedo, A.F.M.; Antunes, J.A.B., "Design methods for steel fiber reinforced concrete industrial floors", Third International Conference Construction Materials: Performance, Innovations and Structural Implications, Vancouver, CD, 22-24, August, 2005. http://hdl.handle.net/1822/5053.
[3] Silfwerbrand, "Design of Steel fiber reinforced concrete slabs on grade for restrained loading", Sixth RILEM Symposium on Fiber-Reinforced Concretes (FRC) By Marco Di Prisco, Giovanni A. Plizzari, Felicetti Roberto, 975-984, 2004.
[4] Destrée, X., "Structural application of steel fibers as only reinforcing in free suspended elevated slabs: conditions – Design examples", Sixth RILEM Symposium on fiber reinforced concrete Varenna/Italy, 2, 1073-1082, September, 2004.
[5] Espion, B., "Test report n°33396", University of Brussels, Belgium, 2004.
[6] Mandl, J., "Flat slabs made of steel fibre reinforced concrete (SFRC)", CPI worldwide, 1, 2008.
[7] Sasani, M.; Sagiroglu, S., "Progressive collapse of reinforced concrete structures: a multihazard perspective", ACI Structural Journal, 105(1), 96-105, January/February, 2008.
[8] FIB-BULLETIN 12, "Punching of structural concrete slabs", Fédération internationale du béton, fib, Lausanne, 2001.
[9] Shaaban, A.M.; Gesund, H., "Punching shear strength of steel fiber reinforced concrete flat plates", ACI Structural Journal, 91(4), 406-414, Jul/Aug, 1994.
[10] Harajli, M.H.; Maalouf D.; Khatib, H., "Effect of fibers on the punching shear strength of slab-column connections", Cement & Concrete Composites, 17(2), 161-170, 1995.
[11] Holanda, K.M.A., "Analysis of the mechanisms provided by steel fibres for the load carrying capacity and ductility performance of concrete slabs failing in punching", PhD Thesis, São Carlos, Brazil, 2002. (in Portuguese).
[12] Muttoni, A.; Ruiz, M.F, "The critical shear crack theory as mechanical model for punching shear design and its application to code provisions", Fédération Internationale du Béton, Bulletin 57, Lausanne, Switzerland, 31-60, 2010.
[13] Model Code 2010, Final draft, CEB-FIP, 2011.

[14] ACI 318, "Building Code Requirements for Structural Concrete", American Concrete Institute, Farmington Hills, Michigan, 2008.
[15] Alexander, S.D.B.; Simmonds, S.H., "Bond model for concentric punching shear", ACI Structural Journal, 89(3), 325-334, May/June, 1992.
[16] Voo, J.Y.L.; Foster, S.J., "Tensile fracture of fibre reinforced concrete: variable engagement model", Sixth Rilem Symposium on Fibre Reinforced Concrete (FRC), Varenna, Italy, 875-884, September, 2004.
[17] Moraes-Neto, B.N.; Barros, J.A.O.; Melo, G., "Data base for the assessment of the predictive performance of design models for the punching resistance of SFRC slabs", Technical Report 12-DEC/E-03, University of Minho, January, 2012. (in Portuguese).
[18] Collins, M.P., "Evaluation of shear design procedures for concrete structures", A Report prepared for the CSA technical committee on reinforced concrete design, 2001.